Western Region Technical Attachment
No. 91-33 (Revised)
August 20, 1991

THUNDERSTORM DEVELOPMENT AT INTERSECTING OUTFLOW BOUNDARIES

[Editor's Note: This Technical Attachment was originally issued last week (August 13, 1991). We later discovered that portions of two sentences in paragraph five were missing in the final version. This is a corrected copy. Please combine this text with the figures sent out with last week's version.]

In summertime convective situations, when the atmosphere is convectively unstable, it is often difficult to pinpoint where individual cells will form during the afternoon hours. One triggering mechanism for cell development is convergent surface winds associated with outflow boundaries from other convective cells. In the Western Region, where surface observations are relatively sparse, these outflow boundaries often are undetected. However, visual satellite imagery sometimes provides excellent indications of these outflow boundaries.

Figure 1 shows a SKEW-T representation of the radiosonde observation from Winslow, AZ (INW) on the morning of August 6, 1991. Analysis of this sounding shows that once a convective temperature of approximately 75°F is reached, saturated parcels could rise spontaneously from the lifted condensation level (near 650mb) all the way to the tropopause (near 200mb). Figure 2 shows weak southwesterly flow at 500mb across this area at the same time, and shows little evidence of any short wave features that might set off convection. However, southwesterly flow across the topography in this area is upslope and this lifting was enough to generate some convective cells by early afternoon.

Figure 3 shows visible satellite images starting from 1800 UTC on August 6 (1100 local time in Arizona). Convective cells are evident in southeastern Utah and southwestern Colorado. One cell with enhanced infrared tops cooler than -30°C is evident in extreme northwest Arizona. The arrow in the image points to an arc-shaped outflow boundary to the south of this cell. This outflow had spread out from this cell over the previous two hours. An hour before this image, winds at Farmington, New Mexico (just across the border with Arizona in the vicinity of this outflow) were northeast at 4 knots, but shifted to west at 16 knots gusting to 24 knots 15 minutes before this image was taken.

In the 1931 UTC satellite image (90 minutes later), the outflow from the cell over southern Utah is harder to distinguish, but still exists a little further south over northeastern Arizona and is indicated by one of the arrows. Animation of satellite images makes it much easier to identify the movement of this boundary. Another cell with enhanced infrared tops has formed further south in eastern Arizona, and an outflow boundary from this cell can be seen moving to the north and west.

By 2101 UTC (90 minutes later), the enhanced infrared tops from the cell over eastern Arizona have moved quickly into New Mexico, but the circular shaped outflow boundary remains. The northern edge of this boundary has reached the southerly remains of the other outflow boundary. The arrow in this image points to the intersection of the outflow boundaries where a new cell has formed with tops already cooler than -30°C.

One hour later, the 2201 UTC image shows that the tops of this cell have cooled to -55°C and it has moved slowly into New Mexico. Note that the tropopause temperature at Winslow from the morning sounding (see Fig. 1) was near -55°C.

The visible satellite images of these outflow boundaries provided a unique clue to surface wind fields in the area. These surface wind fields can interact with local topographic features, the ambient wind field or, as in this case, each other to produce surface convergent wind zones where new convective cells are likely to generate. Animation of visible satellite images (available in most offices by SWIS or MicroSWIS) is particularly valuable in identifying thunderstorm outflow boundaries.

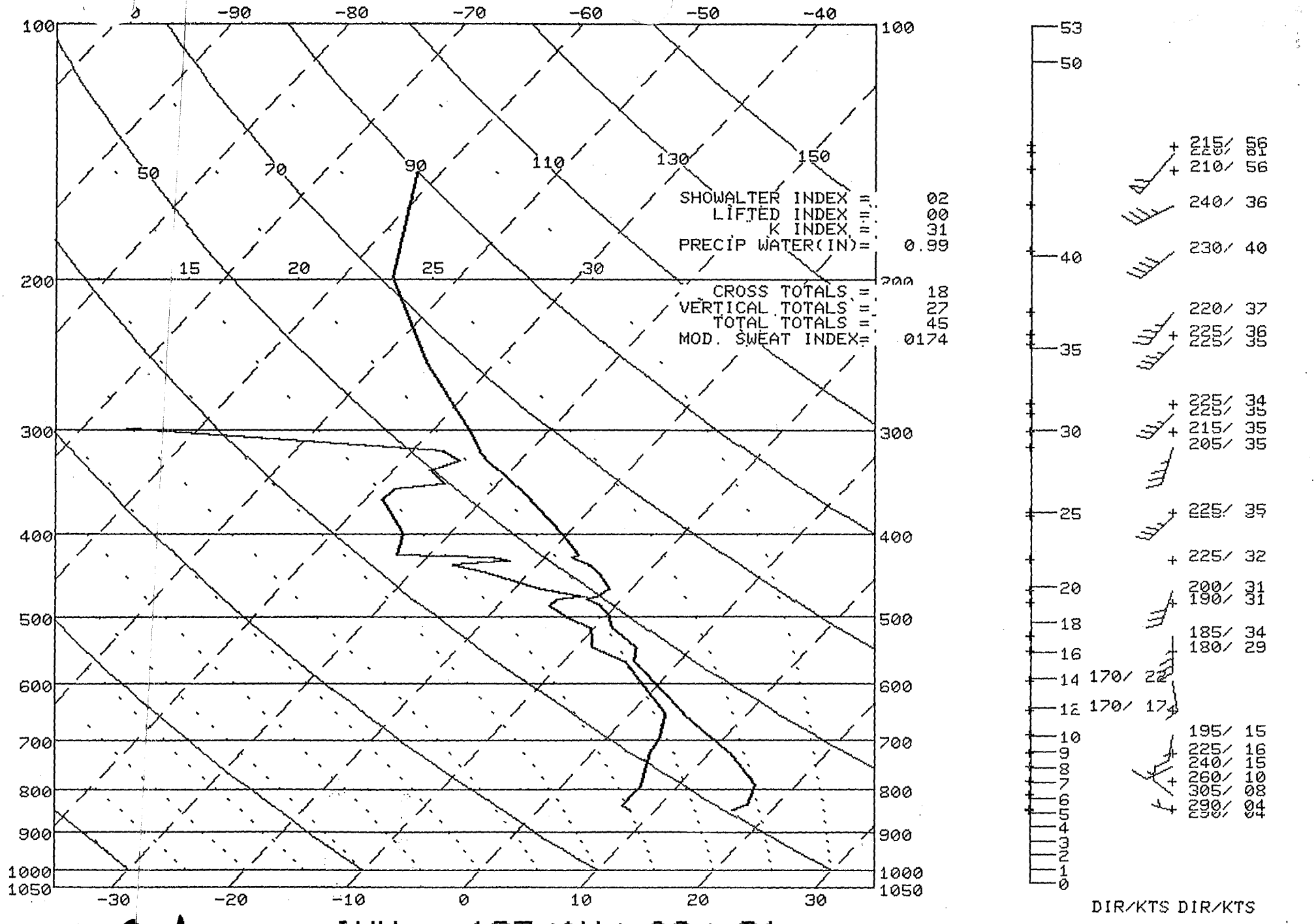

FIG 1

INW 12Z/AU/ 06/ 91

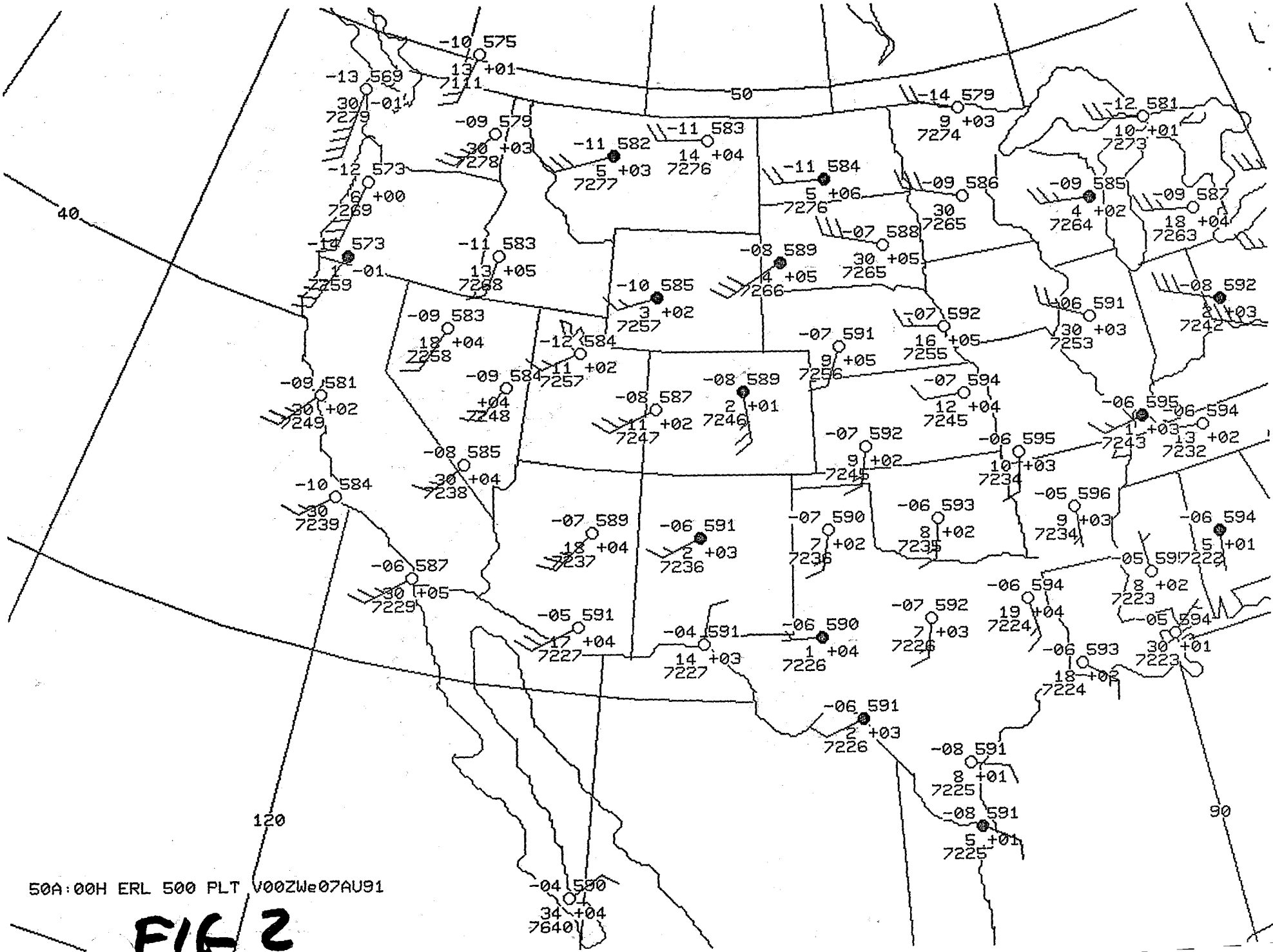

FIG 2

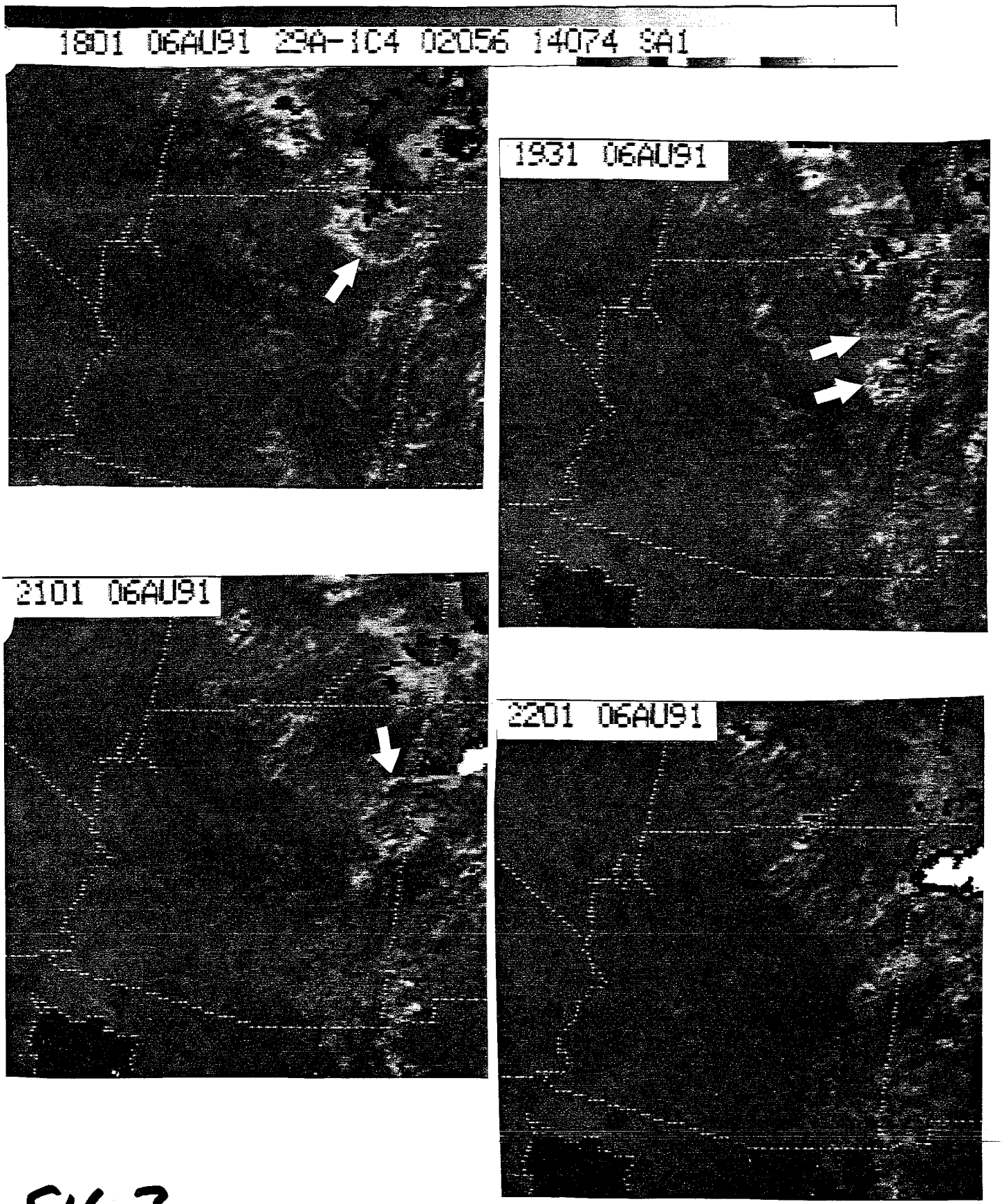
1801 06AU91 23A-1C4 02056 14074 3A1
1931 06AU91
2101 06AU91
2201 06AU91

FIG 3